

PACS number(s): 71.70.Ch

## CRYSTAL ELECTRIC FIELD EFFECT IN $RT_xX_2$ COMPOUNDS

A. Gil

*Faculty of Mathematical and Natural Sciences, JD University,  
Al. Armii Krajowej 13/15, 42-200 Częstochowa, Poland*

The  $RT_xX_2$  type metallic compounds where R is a rare-earth element, T is a d-electron element and X is a p-electron element ( $X = \text{Si, Ge, Sn}$ ) crystallize in the orthorhombic crystal structure of the  $\text{CeNiSi}_2$  type.

The systems discussed exhibit complex magnetic behaviour. Their magnetism arises from the long range interaction of the magnetic moments localized on the rare-earth ions, probably those described by RKKY model. The magnetic ordering in these systems is not purely of the RKKY-type but is modified by the crystalline electric field effect, which can significantly influence the magnitude of the Néel temperature. The CEF effects are also responsible for the observed decrease in the rare-earth magnetic moments as compared with the free ion values.

The determination of the CEF parameters is important for understanding the nature of magnetic properties of intermetallic compounds. The  $B_n^m$  parameters were calculated for  $RTX_2$  compounds using the so-called point-charge model. The quadrupole splitting observed in the Mössbauer spectra of  $\text{GdT}_x\text{Sn}_2$  compounds ( $T = \text{Fe, Co, Ni, Cu}$ ) allow to determined the experimental values of  $B_2^0$  parameters for  $RTX_2$  compounds.

*Key words:* crystal field, magnetic properties.

During the last few years the  $RT_xX_2$  ( $x \leq 1$ ) type intermetallic compounds (R is a rare-earth, T is a d-electron metal and X is a p-electron metalloid ( $X = \text{Si, Ge, Sn}$ )) have been a subject of intensive studies because of their intriguing physical properties, which have both fundamental and practical significance.

The  $RT_xX_2$  compounds crystallize in different orthorhombic crystal structures [1]:

- $\text{CeNiSi}_2$ -type (space group Cmc<sub>2</sub>m);
- $\text{TbFeSi}_2$ -type, which is very similar to the  $\text{CeNiSi}_2$ , but R, T and Si atoms are located in alternating layers;
- $\text{YIrGe}_2$ -type (space group Immm);
- $\text{LuNiSn}_2$ -type (space group Pnma);
- $\text{TiMnSi}_2$  or  $\text{ZrCrSi}_2$ -type (space group Pbam);
- $\text{NdRuSi}_2$ -monoclinic type, which is described as a distorted variant of the  $\text{CeNiSi}_2$ -type (space group P2<sub>1</sub>/m).

All silicides crystallize in the stoichiometric structure ( $x=1$ ), while germanides and stannides form mainly defected structures  $RT_xX_2$  ( $x<1$ ) with defects in d-electron metal sublattice.

Majority of these compounds crystallize in the orthorhombic  $CeNiSi_2$ -type structure [2] (Fig. 1) and discussion in this work concerns compounds with this structure type.

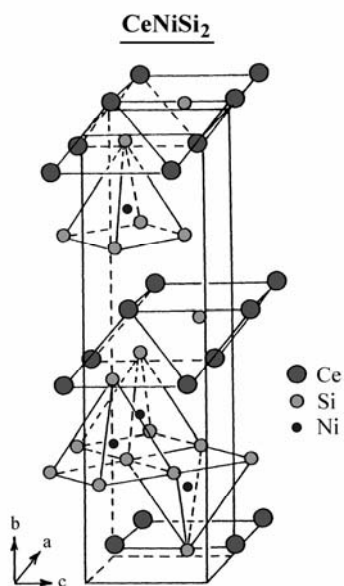


Fig. 1. Crystal structure of  $CeNiSi_2$ -type

Magnetic measurements indicate that majority of compounds order antiferromagnetically at low temperatures. Above the Néel temperatures, the effective magnetic moments are close to the free  $R^{3+}$  ion values ( $g\sqrt{J(J+1)}$ ). Only for compounds with  $T = Mn$ , a localized magnetic moment on Mn has been observed (Fig. 2).

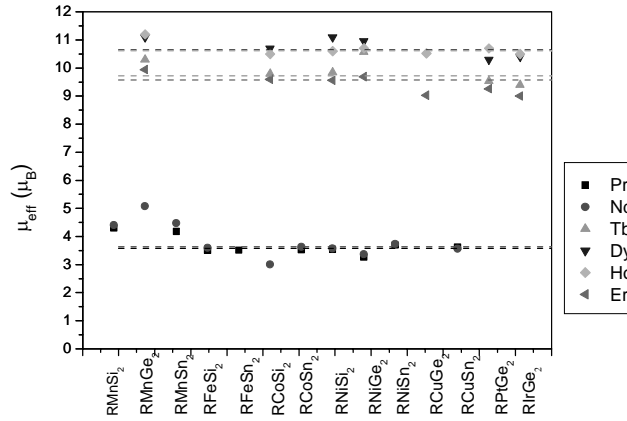


Fig. 2. Effective magnetic moments for  $RT_xX_2$  compounds

The crystal structure has a distinct layer character. Rare-earth atoms occupy the layers perpendicular to the b-axis, and they are separated by layers of other atoms. In majority of compounds, the magnetic moments located in the same planes are coupled ferromagnetically, while the coupling between two moments in adjacent planes is antiferromagnetic.

Magnetic data for the  $RT_xX_2$  ternary compounds are summarized in Table 1.

Table 1

Magnetic properties of  $RT_xX_2$  compounds

Compound	TMO <sup>1</sup>	$\theta_p$ [K]	$\mu_{\text{eff}}$ [ $\mu_B$ ]	$T_{C,N}$ [K]	$\mu_R$ [ $\mu_B$ ]	MMD <sup>2</sup>	Ref.
CeMnSi <sub>2</sub>	F	420	3,52	398	0,23	<i>b</i>	3,4
PrMnSi <sub>2</sub>	F	450	4,29	434,34	2,04	<i>b</i>	3,4
NdMnSi <sub>2</sub>	F	460	4,41	441,40	1,8	<i>c</i>	3,4
SmMnSi <sub>2</sub>	F	482	3,02	464	1,74		3
NdMn <sub>0,42</sub> Ge <sub>2</sub>	AF	-23,5	5,08	34	1,55	<i>c</i>	5
SmMn <sub>0,4</sub> Ge <sub>2</sub>		-57,2	3,7				5
GdMn <sub>0,38</sub> Ge <sub>2</sub>	AF	-30,5	8,75	35			5
TbMn <sub>0,33</sub> Ge <sub>2</sub>	AF	-37,1	10,3	26	7,0	<i>c</i>	5
DyMn <sub>0,32</sub> Ge <sub>2</sub>	AF	-17,8	11,1	30			5
HoMn <sub>0,33</sub> Ge <sub>2</sub>	AF	-12,8	11,2	7	7,3	<i>c</i>	5
ErMn <sub>0,27</sub> Ge <sub>2</sub>	AF	-10,7	9,95	3,4			5
CeMnSn <sub>2</sub>	F	117	4,03	320	0,4		6
CeMn <sub>0,5</sub> Sn <sub>1,83</sub>	F	369	3,8	520	0,55		6
PrMn <sub>0,5</sub> Sn <sub>1,83</sub>	AF	-14	4,18	16	3,09	<i>c</i>	7

NdMn <sub>0,5</sub> Sn <sub>1,83</sub>	AF	-39	4,48	20			6
SmMn <sub>0,29</sub> Sn <sub>1,56</sub>	AF	-105	1,97	35			6
PrFeSi <sub>2</sub>	F	44	3,5	26	2,58	<i>b</i>	3, 8
NdFeSi <sub>2</sub>	AF	41	3,6	6	3,17	<i>b</i>	3, 8
CeFe <sub>0,63</sub> Ge <sub>2</sub>	NM Kondo	-115	2,8				9
CeCoSi <sub>2</sub>	PP	-240	1,6				10
NdCoSi <sub>2</sub>	AF	-28	3,0	2,15	2,18		11, 12
SmCoSi <sub>2</sub>	AF			4			11
GdCoSi <sub>2</sub>	AF	-8	7,5	7,5			11
TbCoSi <sub>2</sub>	AF	-18	9,8	16	9,16	<i>a</i>	11, 13
DyCoSi <sub>2</sub>	AF	8	10,7	10	5,74	( <i>a-c</i> )	11, 14
HoCoSi <sub>2</sub>	AF	-6	10,5	6,3	6,72	<i>a</i>	11, 14
ErCoSi <sub>2</sub>	AF	-17	9,6	2,6	4,63	( <i>a-c</i> )	11, 15
CeCo <sub>0,89</sub> Ge <sub>2</sub>	AF Kondo	-90	2,55	3			9
CeCo <sub>0,48</sub> Sn <sub>2</sub>		-9	2,71				16
PrCo <sub>0,33</sub> Sn <sub>2</sub>		-2	3,52				16
NdCo <sub>0,33</sub> Sn <sub>2</sub>		-7	3,63				16
GdCo <sub>0,27</sub> Sn <sub>2</sub>	AF			16,5			17
TbCo <sub>0,25</sub> Sn <sub>2</sub>	AF			18,8	7,14	( <i>a-c</i> )	17
DyCo <sub>0,26</sub> Sn <sub>2</sub>	AF			7			17
HoCo <sub>0,23</sub> Sn <sub>2</sub>	AF			5,6	6,79	( <i>a-c</i> )	17
ErCo <sub>0,24</sub> Sn <sub>2</sub>	AF			4,7	6,15	( <i>a-c</i> )	18
CeNiSi <sub>2</sub>	MV	-150	2,6				19
PrNiSi <sub>2</sub>	F	20	3,54	20	3,09	<i>c</i>	20
NdNiSi <sub>2</sub>	F	8	3,57	9,5	2,38	<i>c</i>	20
SmNiSi <sub>2</sub>	AF		0,88	9,8			21
GdNiSi <sub>2</sub>	AF	-33	9,4	19,3	5,8		21
TbNiSi <sub>2</sub>	AF	-17	9,84	37,6			21
		-5	10,1	36,2	8,7	<i>c</i>	22
DyNiSi <sub>2</sub>	AF	-12	11,1	25			21
		21	10,6	24	7,5	<i>c</i>	23

HoNiSi <sub>2</sub>	AF	3	10,6	10			21
		3	11,05	10	8,13	<i>c</i>	24
ErNiSi <sub>2</sub>	AF	4	9,56	3,1			21
		20	10,11	3,4	7,6	<i>b</i>	25
CeNiGe <sub>2</sub>	AF HF	-20,8	2,51	3,9, 3,2			19
PrNiGe <sub>2</sub>	F	13,8	3,26	15			21
NdNiGe <sub>2</sub>	F	7	3,31	15			21
		6	3,37	6	2,32	<i>c</i>	26
SmNiGe <sub>2</sub>		-13,6	0,97				21
GdNiGe <sub>2</sub>	AF	-33	8,6	24,5			21
TbNiGe <sub>2</sub>	AF	-31,5	10,57	42	8,8	<i>c</i>	21, 27
				16	5,6	<i>c</i>	28
TbNi <sub>0,4</sub> Ge <sub>2</sub>	AF			31	8,9	<i>c</i>	28
TbNi <sub>0,6</sub> Ge <sub>2</sub>	AF			38	8,7	<i>c</i>	28
TbNi <sub>0,8</sub> Ge <sub>2</sub>	AF						21
DyNiGe <sub>2</sub>	AF	-12	10,96	22			21
HoNiGe <sub>2</sub>	AF	-5	10,71	7,6			21
HoNi <sub>0,64</sub> Ge <sub>2</sub>	AF			11	6,7	<i>c</i>	27
ErNiGe <sub>2</sub>	AF	-2	9,69	2,5			21
ErNi <sub>0,65</sub> Ge <sub>2</sub>	AF			2,5	2,8	<i>a</i>	
CeNiSn <sub>2</sub>	AF	-6,9	2,56	4			19
CeNi <sub>0,84</sub> Sn <sub>2</sub>	AF			4, 3	2,0	<i>c</i>	29
PrNiSn <sub>2</sub>		-2	3,69				16
NdNiSn <sub>2</sub>		-3	3,73				16
GdNi <sub>0,4</sub> Sn <sub>2</sub>	AF			27			30
TbNi <sub>0,26</sub> Sn <sub>2</sub>	AF			17,4	8,05	( <i>a-c</i> )	31
DyNi <sub>0,22</sub> Sn <sub>2</sub>	AF			8	9,2	( <i>b-c</i> )	32
HoNi <sub>0,16</sub> Sn <sub>2</sub>	AF			6,6	7,46	( <i>a-c</i> )	31
ErNi <sub>0,15</sub> Sn <sub>2</sub>	AF			4	9,16	<i>a</i>	18
CeCu <sub>0,86</sub> Ge <sub>2</sub>	AF	7		15,6			19
				16,5	1,85	<i>c</i>	33
PrCu <sub>0,76</sub> Ge <sub>2</sub>	F			23			34
TbCu <sub>0,4</sub> Ge <sub>2</sub>	AF	-25	10,4	39	8,82	<i>c</i>	35
HoCu <sub>0,33</sub> Ge <sub>2</sub>	AF	-8,0	10,52	8	8,18	<i>c</i>	36
ErCu <sub>0,25</sub> Ge <sub>2</sub>	AF	4,1	9,03	4,5	7,89	<i>a</i>	36
CeCu <sub>0,62</sub> Sn <sub>1,83</sub>		1	2,4				16
PrCu <sub>0,62</sub> Sn <sub>1,83</sub>		10	3,62				16
NdCu <sub>0,74</sub> Sn <sub>1,96</sub>		-6	3,8				16

<sup>1</sup> TMO –type of magnetic ordering, <sup>2</sup> MMD –magnetic moment direction

In all series of compounds, the  $R^{3+}-R^{3+}$  distances are large (about 4 Å), suggesting that direct magnetic interactions are highly improbable. The stability of the observed magnetic ordering schemes may be considered as being due to interactions via conduction electrons described by the RKKY model [37–39].

In this mechanism, the ordering temperature should be proportional to the de Gennes factor [40]:  $G = (g_J - 1)^2 J(J + 1)$ , where  $g_J$  is the Landé factor and  $J$  — the total angular momentum of the rare-earth ion, and the highest ordering temperature should be found in the Gd-containing compounds. Contrary to the latter expectation, in majority of our systems, the  $T_N(G)$  dependence is peaked around the value of  $G$  corresponding to terbium. (Fig. 3). The  $T_{C,N}$  shifting may result from the crystalline electric field effect CEF. This is why the CEF terms should be added to the exchange Hamiltonian. The rare earth ions are in the  $4(c)$  site of the low symmetry  $mm$ . Neither experimental nor calculated data concerning CEF parameters for  $RT_xX_2$  are available.

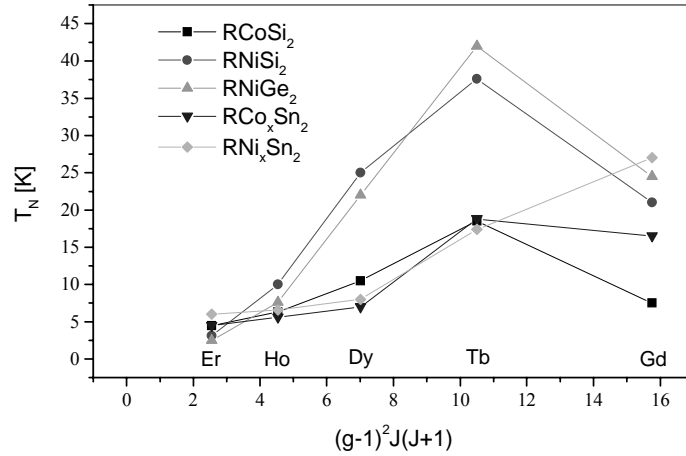


Fig. 3. Observed Néel temperatures in some  $RT_xX_2$  intermetallics vs de Gennes function

The interaction of the CEF with the moments of rare-earth atom electrons is given by the Hamiltonian [41]:

$$H_{CF} = \sum_{n=0}^{n'} \sum_{m=-n}^{+n} B_n^m O_n^m(J),$$

where  $n'$  takes a maximum value of  $n$  appropriate to the rare-earth atom considered,  $B_n^m$  are the crystal field intensity parameters and  $O_n^m(J)$  represent polynomials of the angular momentum operators  $J_+$ ,  $J_-$ ,  $J_z$  and  $J^2$ .

The rare-earth site in the  $RTX_2$  compounds has the point symmetry  $mm$ . In such symmetry the CEF Hamiltonian can be written as follows:

$$H_{CF} = B_2^0 O_2^0 + B_2^2 O_2^2 + B_4^0 O_4^0 + B_4^2 O_4^2 + B_6^0 O_6^0 + B_6^2 O_6^2 + B_6^4 O_6^4 + B_6^6 O_6^6.$$

When  $B_2^0$  is the leading term in the crystal field Hamiltonian, then its sign gives information about the single ion magnetic anisotropy. For a positive value of the  $B_2^0$  parameter the basal plane ( $\perp z$ ) is preferred for the magnetic moment direction while for a negative value an ordering along  $z$ -axis is anticipated [42].

The neutron diffraction data collected in Table 1 indicate that the rare-earth magnetic moments in  $\text{RTX}_2$  compounds prefer the orientation in the basal plane (010). In majority of  $\text{RTX}_2$  compounds with  $R = \text{Pr, Nd, Tb, Ho}$ , the rare-earth moments are parallel to the  $c$ -axis and for  $R = \text{Er}$  the magnetic moment is parallel to the  $a$ -axis.

The  $B_n^m$  parameters were determined for  $\text{RTX}_2$  compounds using the so-called point-charge model [43] taking  $b$ -axis as  $z$ -axis and  $c, a$ -axes as  $x, y$ -axes respectively. In this approximation the electrostatic potentials of the most important neighbours are summed. The parameters  $B_n^m$  can be written as:

$$B_n^m = \langle \theta_n \rangle \langle r^n \rangle K_n^m A_n^m .$$

Values for  $\langle \theta_n \rangle \langle r^n \rangle$  have been collected by Franse and Radwański [44]. The coefficients  $A_n^m$  are known as the CEF coefficients.

The computations were made for the nearest neighbours (see Fig. 4). The  $B_2^0$ ,  $B_2^2$  and  $B_4^0$  parameters are given by the formulas:

$$B_2^0 = -\alpha_J \langle r^2 \rangle \frac{\pi e^2}{20} \sum_i \frac{Z_i}{R_i^3} (3 \cos^2 \theta - 1);$$

$$B_2^2 = -\alpha_J \langle r^2 \rangle \frac{\pi e^2}{10} \sum_i \frac{Z_i}{R_i^3} \sin^2 \theta (2 \cos^2 \varphi - 1);$$

$$B_4^0 = -\beta_J \langle r^4 \rangle \frac{4\pi e^2}{9} \sum_i \frac{Z_i}{R_i^5} (35 \cos^4 \theta - 30 \cos^2 \theta + 3) \dots$$

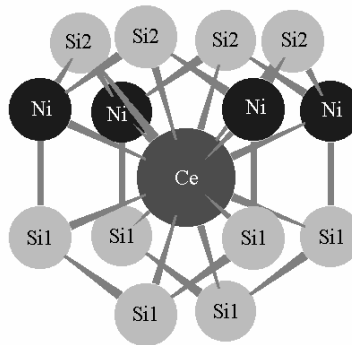


Fig. 4. The nearest neighbours of a rare atom in the  $\text{RTX}_2$  compounds

The results of calculations of  $B_n^m$  are shown in Table 2 (the sixth-order parameters were omitted because they are very small). The calculations suggest that the preferred direction of magnetic moment occurs in the plane (010) as well as that the  $B_2^0$  and  $B_2^2$  and  $B_4^0$  parameter play an important role in the CEF Hamiltonian.

Table 2

Crystalline electric field parameters for RNiSi<sub>2</sub> compounds calculated using the so-called point-charge model

R	$B_2^0$ [meV]	$B_2^2$ [meV]	$B_4^0$ [meV]	$B_4^2$ [meV]	$B_4^4$ [meV]
Ce	2,741	9,445	6,979	-0,229	-0,257
Pr	0,907	3,126	-0,656	0,022	0,024
Nd	0,256	0,882	-0,222	0,007	0,008
Tb	0,307	1,058	0,055	-0,002	-0,002
Dy	0,184	0,634	-0,025	0,001	0,001
Ho	0,061	0,209	-0,012	0,0004	0,0004
Er	-0,067	-0,231	0,014	-0,0005	-0,0005

In the most of studied compounds with the CeNiSi<sub>2</sub> – type crystal structure the orientation of magnetic moments agree with the positive sign of the  $B_2^0$  parameter (along the *c*-axis) but for the compounds with Er the negative sign of  $B_2^0$  parameter suggests the *b*-axis as the preferable direction.

It has been also found that a decrease in the number of defects in the Ni sublattice leads to an increase of the  $B_2^0$  parameter and to a reduction of the  $B_2^2$  parameter (see Table 3).

Table 3

Influence of Ni sublattice defects in CeNi<sub>x</sub>Si<sub>2</sub> on the CEF parameters

	$B_2^0$ [meV]	$B_2^2$ [meV]	$B_4^0$ [meV]	$B_4^2$ [meV]	$B_4^4$ [meV]
CeNiSi <sub>2</sub>	2,741	9,445	6,979	-0,229	-0,257
CeNi <sub>0,75</sub> Si <sub>2</sub>	4,339	9,296	6,875	-0,229	-0,244
CeNi <sub>0,5</sub> Si <sub>2</sub>	5,936	9,147	6,771	-0,230	-0,232
CeNi <sub>0,25</sub> Si <sub>2</sub>	7,533	8,998	6,667	-0,230	-0,220
CeSi <sub>2</sub>	9,130	8,849	6,563	-0,230	-0,208

The samples of gadolinium stannides GdT<sub>x</sub>Sn<sub>2</sub> (T = Fe, Co, Ni and Cu) have been studied by <sup>119</sup>Sn and <sup>155</sup>Gd Mössbauer spectroscopy [45].

Since the trivalent gadolinium ions are in the ground electronic states with spherical distribution of *4f* electronic charge, only the lattice term contributes to the magnitude of  $V_{zz}$  in the rare earth site. Hence, the determination of the sign and magnitude of  $\Delta E_Q = eV_{zz}Q$  at the Gd site together with the asymmetry parameter  $\eta$  allow



to estimate the quadrupolar terms  $B_2^0$  and  $B_2^2$  in Stevens expansion of the crystal field Hamiltonian, as they are related by two simple formulas:

$$B_2^0 [K] = -\alpha_J \cdot \langle r^2 \rangle_{4f} \cdot 90,2 \cdot \Delta E_Q (^{155}Gd), \quad B_2^2 = \eta B_2^0.$$

Here,  $\alpha_J$  is the appropriate Stevens factor, the mean squared radius of the  $4f$  wave function  $\langle r^2 \rangle_{4f}$  is expressed in atomic units and  $\Delta E_Q$  in mm/s.

Görlich et al. [45] determined  $\Delta E_Q = -0,32$  mm/s for  $GdNi_{0.32}Sn_2$  compound and I tried to determine the  $B_2^0$  parameters for  $RNi_xSn_2$  compounds which are shown in Table 4.

Table 4

 $B_2^0$  parameters for  $RNi_xSn_2$  compounds

R	Ce	Pr	Nd	Tb	Dy	Ho	Er
$B_2^0$ [meV]	-0,640	-0,219	-0,061	-0,071	-0,043	-0,014	0,016

These results indicate that the change of the X element from Si to Sn may leads to a change in the direction of the magnetic moments. Another reason for a change of  $B_2^0$  signs maybe a non stoichiometry of stannides.

The discussed compounds crystallize in the orthorhombic crystal structures of the  $CeNiSi_2$  type. The silicides form stoichiometric compounds while germanides and stannides show mainly non stoichiometric structures.

It is well established now that in these compounds (except those with T=Mn) the magnetic moment is localized only on the rare-earth atoms. Their magnetism arises from the interaction of the magnetic moments localized on the rare-earth ions.

The large interatomic R-R distances (about 4 Å) and the appearance of complex magnetic structures suggest that long-range magnetic ordering, realized probably by conduction electrons (RKKY model) play a dominant role in forming the magnetic ordering.

The Néel and Curie temperatures determined for presented families only in part follow the de Gennes scaling. This effect suggests that the main interaction is not purely of the RKKY-type but is modified by the crystalline electric field effect, which generally can enhance or even decrease the magnitude of the Néel temperature and is also responsible for the observed decrease in the rare-earth magnetic moments as compared with the free ion values.

The calculations of CEF parameters suggest that the preferred direction of magnetic moment occurs in the plane (010) as well as that the  $B_2^0$  and  $B_2^2$  and  $B_4^0$  parameter play an important role in the CEF Hamiltonian. In the most of studied compounds the orientations of magnetic moments agree with the positive sign of the  $B_2^0$  parameter (along the  $c$ -axis).

1. *Parthé E., Chabot B.* Handbook on the Physics and Chemistry of Rare Earth, eds. K. A. Gschneidner Jr and L. Eyring; Elsevier Science Publ. B. Vol. Chap. 48. 1984. 113 p.
2. *Bodak O. I., Gladyshevsky E. I.* Sov. Phys. Cryst. 1970. Vol. 14. 859 p.
3. *Venturini G., Malaman B., Meot-Meyer M.* et al. Revue de Chimie Minerale. 1986. Vol. 23. 162 p.
4. *Malaman B., Venturini G., Pontonnier L., Fruchart D.* J. Magn. Magn. Mater. 1990. Vol. 86. 349 p.
5. *Gil A., Leciejewicz J., Maletka K., Szytuła A.* et al. J. Magn. Magn. Mater. 1994. Vol. 129. L. 155.
6. *Weitzer F., Hiebel K., Rogl P.* Solid State Commun. 1992. Vol. 82. 353 p.
7. *Gil A., Oleś A., Sikora W., Szytuła A.* J. Alloys Comp. 2003. Vol. 360. 21 p.
8. *Malaman B., Venturini G., LeCaër G., Pontonnier L.* et al. Phys. Rev. B41. 1990. 4 700 p.
9. *Das I., Sampathkumaran E. V.* Solid State Commun. 1992. Vol. 83. 765 p.
10. *Bodak O. I., Gladyshevsky E. I., Levin E. M., Lutsiv R. V.* Dopov. Akad. Nauk Ukr. RSR. Ser. A12. 1977. 1129 p.
11. *Pellizzone M., Braun H. F., Muller J. J.* Magn. Magn. Mater.; 1982. Vol. 30. 33 p.
12. *André G., Oleś A., Szytuła A.* Phys. Stat. Solidi. 1989. Vol. 116. K. 29.
13. *Penc B., Szytuła A., Wawrzyńska E., Hernandez-Velasco J. J.* Alloys Comp. 2004. Vol. 366. 120 p.
14. *Szytuła A., Ptasiwicz-Bąk H., Leciejewicz J., Bażela W.* J. Magn. Magn. Mater. 1989. Vol. 80. 189 p.
15. *André G., Bourée F., Oleś A., Sikora W.* et al. J. Magn. Magn. Mater. 1993. Vol. 124. 69 p.
16. *Skolozdra R. V.* Handbook on the Physics and Chemistry of Rare Earths. eds. K. A. Gschneidner and L. Eyring. 1997. Vol. 24. 399 p.
17. *Gil A., Penc B., Wawrzyńska E., Hernandez-Velasco J., Szytuła A., Zygmunt A. J.* Alloys Comp. 2004. Vol. 365. 31 p.
18. *Penc A., Wawrzyńska E., Szytuła A., Gil A., Hernandez-Velasco J., Zygmunt A.* J. Alloys Comp. 2004. Vol. 375. L1.
19. *Pellizzone M., Braun H. F., Muller J. J.* Magn. Magn. Mater. 1982. Vol. 30. 33 p.
20. *Schobinger-Papamantellos P., Buschow K. H. J. J.* Alloys Comp. 1992. Vol. 18. 551 p.
21. *Gil A., Szytuła A., Tomkowicz Z., Wojciechowski K.* et al. J. Magn. Magn. Mater. 1994. Vol. 129. 271 p.
22. *Schobinger-Papamantellos P., Buschow K. H. J. J.* Less-Common Met. 1991. Vol. 171. 321 p.
23. *Schobinger-Papamantellos P., Ritter C., Buschow K. H. J. J.* Alloys Comp. 1998. Vol. 264. 89 p.
24. *Schobinger-Papamantellos P., Fauth F., Buschow K. H. J. J.* Alloys Comp. 1997. Vol. 252. 50 p.
25. *Schobinger-Papamantellos P., Buschow K. H. J.* et al. J. Magn. Magn. Mater. 1998. Vol. 189214.
26. *Schobinger-Papamantellos P., Krimmel A., Grauel A., Buschow K. H. J. J.* Magn. Magn. Mater. 1993. Vol. 125. 151 p.
27. *Bażela W., Leciejewicz J., Maletka K., Szytuła A.* J. Magn. Magn. Mater. 1992. Vol. 109. 305 p.

28. *Schobinger-Papamentellos P., Buschow K. H. J., Ritter C. J.* Alloys Comp. 1999. Vol. 287. 51 p
29. *Schobinger-Papamantellos P., Rodriguez-Carvajal J., Buschow K.H.J.* J. Alloys Comp. 1996. Vol. 240. 85 p.
30. *Gil A., Penc B., Baran S., Hernandez-Velasco J., Szytula A., Zygmunt A.* J. Alloys Comp. 2003. Vopl. 361. 32 p.
31. *Gil A., Penc B., Baran S., Wawrzyńska E., Szytula A.* et al. Neutron Scattering and Complementary Methods in Investigations of Condensed Phase, Vol. 1, University of Podlasie Publishing House. 2003. Monograph. N 45, 103 p.
32. *Gil A., Penc B., Hernandez-Velasco J., Szytula A., Zygmunt A.* Physica B. 2004. Vol. 350. e119.
33. *Gil A., Penc B., Gondek L., Szytula A., Hernandez-Velasco J.* J. Alloys Comp. 2002. Vol. 346. 43 p.
34. *Rawat R., Das I.* Phys. Rev. 2001. Vol. B64.
35. *Schobinger-Papamentellos P., Buschow K.H.J.* J. Alloys Comp. 1992. Vol. 187. 73 p.
36. *Gil A., Kaczorowski D., Hernandez-Velasco J., Penc B.* J. Alloys Comp. 2004. Vol. 384. L4.
37. *Ruderman M. A., Kittel C.* Phys. Rev. 1954. Vol. 96. 99 p.
38. *Kasuya T.* Prog. Theor. Phys. (Kyoto); 1956. Vol. 16. 45 p.
39. *Yoshida K.* Phys. Rev. 1957. Vol. 106. 893 p.
40. *Gennes de P. G.* J. Phys. Radium: 23. 1962. Vol. 510. 630 p.
41. *Stevens K. W. H.* Proc. Phys. Soc. Londyn. A65. 1952. 209 p.
42. *Wallace W.E., Sankar S.G., Rao V.U.S.* Crystal field effects in rare-earth intermetallic compounds, in: Structure and Bonding. Berlin. Vol. 33. 1997.
43. *Hutchings M.T.* Solid State Physics. Vol.16. F. Seits, D. Turnbull Eds.; Academic Press, New York. 1964. 227 p.
44. *Franse J.J. M. anRadwanski d R.J.* Handbook of Magnetic Materials. Vol. 7. Ed. K. H. J. Buschow. 1993. 307 p.
45. *Görlich E.A., Łątka K., Kmiec R., Tomkowicz Z., Warkocki W.* Molecular Physics Reports. 2000. Vol. 30. 59 p.

**ЕФЕКТ КРИСТАЛІЧНОГО ПОЛЯ В СПОЛУКАХ ТИПУ  $RT_xX_2$** **А. Гіл**

*Факультет математики і природничих наук, університет імені Яна Длугоша  
вул. Армії Крайовей 13/15, 42-200 Ченстохова, Республіка Польща*

У статті досліджено сполуки  $RT_xX_2$  (R – рідкоземельні елементи, T – елементи з валентними *d*-електронами, X – елементи з *p*-електронами), що мають ромбічну структуру типу  $CeNiS_2$ .

Розраховані параметри  $B_n^m$  для  $RT_xX_2$  сполук у разі використання моделі точкового заряду. Простежено в Месбауерівських спектрах  $GdT_xSn_2$  (T = Fe, Co, Ni, Cu) квадрупольне розщеплення дало змогу з'ясувати величину параметра  $B_2^0$  для сполук  $RT_xX_2$ .

*Ключові слова:* кристалічне поле, магнітні властивості.

Стаття надійшла до редколегії 29.05.2006  
Прийнята до друку 26.02.2007